An Adaptive-Focusing Algorithm for a Microwave Planar Phased-Array Hyperthermia System

Alan J. Fenn, Chris J. Diederich, and Paul R. Stauffer

■ We have experimentally investigated the use of adaptive-focusing techniques in the hyperthermia treatment of cancer. Gradient-search adaptive-focusing software developed at Lincoln Laboratory has been implemented on a commercial microwave hyperthermia planar phased-array antenna system at the University of California at San Francisco (UCSF). The system, manufactured by Labthermics Technologies, Inc., consists of 16 independent amplitude/phase-controlled waveguide antenna elements operating at 915 MHz.

In the experiments, conducted at UCSF, a method of steepest-ascent gradient-search feedback algorithm was used to control the hyperthermia array phase shifters and focus the transmitted radiation beam at a hypothetical tumor site in a muscle-equivalent sugar/saline liquid phantom. A feedback probe, embedded in the phantom, measured the resulting electric field (E-field) generated by the antenna array. The measured data indicate a significant increase in the focal-region field strength with a rapid convergence of the adaptive-focusing algorithm in 10 to 15 iterations. From the measurements, the maximum useful heating depth in the sugar/saline phantom is estimated for the 915-MHz system at about 3 cm.

Adaptive array antennas are well known for their ability to improve, in real time, the performance of communications and radar systems [1–4]. Recently, adaptive array techniques have been applied in the medical field for the hyperthermia treatment of deep-seated tumors [5–12]. (For an introduction to hyperthermia treatment, see the box, "Treating Cancer with Hyperthermia," on the following page.) With an adaptive radio frequency (RF) or microwave hyperthermia array, it is possible to control the electric field (E-field) automatically at multiple positions within the target body [5–12]. The E-field radiated by a hyperthermia phased array can be minimized (nulled) and maximized (focused) at desired target positions by adaptively adjusting the transmit amplifiers and phase shifters of the hyperthermia apparatus. Multiple adaptive E-field nulls and adaptive focusing were experimentally demonstrated at the State University of New York (SUNY) Health Science Center on a modified commercial RF hyperthermia system. In the experiments, gradient-search software, developed at Lincoln Laboratory, was used to control the generated E-field of the Sigma-60 (manufactured by BSD Medical Corp. of Salt Lake City, Utah), an annular phased-array antenna system operating at approximately 100 MHz [9–14]. Details of the SUNY experiments have been reported in an earlier issue of this journal [11].

Subsequent to the SUNY experiments, the same gradient-search algorithm was implemented on a different commercial hyperthermia system—the Microtherm-1000 (manufactured by Labthermics Technologies, Inc., of Champaign, Illinois), a planar phased-array microwave antenna system operating at

TREATING CANCER WITH HYPERTHERMIA

THE TREATMENT OF malignant tumors is often a difficult task. The objective is to reduce or completely remove the tumor mass through the use of one or more modalities, commonly surgery, chemotherapy, and radiation therapy [1]. One particular method used in conjunction with another modality is hyperthermia [1–6], in which a tumor is heated to diminish it.

Hyperthermia treatment requires a controlled thermal dose distribution. Typical localized hyperthermia temperatures that are necessary for the therapeutic treatment of cancer are in the range 42.5° to 45°C. (The normal temperature of human tissue is 37°C.) During treatment, surrounding healthy tissue should be kept at temperatures below 42.5°C. The most difficult aspect of inducing hyperthermia with either electromagnetic or acoustic (ultrasound) waves is producing sufficient heating at the site of a tumor, especially a deep-seated one, without damaging any healthy tissue.

For electromagnetic hyperthermia treatment, multiple-antenna radio frequency (RF) or microwave hyperthermia arrays are commonly used to provide a focused main beam at the tumor site. A focal region should be concentrated at the tumor with minimal energy delivered to the surrounding normal tissue. Because the hyperthermia antenna beamwidth is proportional to the wavelength, a small focal region suggests that the wavelength be as small as possible. Due to propagation losses in tissue, however, the penetration depth decreases with increasing transmit frequency. Typically, for noninvasive phased arrays an operating frequency close to 100 MHz is recommended for the heating of deep-seated tumors and a frequency close to 900 MHz for the heating of shallow tumors.

A typical clinical RF or microwave hyperthermia treatment consists of several two-hour sessions spread over a period of weeks. During the first hour of a session, instrumentation to monitor temperature and other vital signs is attached to the patient. Next, for about 15 minutes, the hyperthermia equipment is turned on and adjusted to achieve the desired temperature in the tumor. The adjustments to the hyperthermia equipment can consist of changes in the transmit power level (for single-antenna devices), or changes in both the transmit power level and phase (for multiple-antenna devices). The tumor is then heated for approximately 45 minutes by radiated electromagnetic energy to a temperature of 42.5° to 45°C. Note that, in order to limit the overall length of the treatment sessions to two hours, only a maximum of 15 minutes is available for adjusting the hyperthermia equipment to achieve the ideal electric field (E-field) distribution for a particular patient.

Current clinical operation of commercial hyperthermia phased-array devices allows limited manual control of the array transmit-antenna amplitude and phase. Although this manual trial-and-error method can achieve some improvement in the E-field distribution, automatic adjustment techniques, such as those offered by adaptive arrays, are desirable because of their promise of faster operation and better E-field distributions.

Several journals have published special issues on the acoustic and electromagnetic hyperthermia treatment of cancer [6–8], and various articles have investigated the widely differing methods for improving such treatment. For example, many studies [7, 9–12] have shown that phased arrays can be used to produce improved therapeutic field distributions: researchers have demonstrated that phase control can synthesize improved RF radiation patterns without adaptive control of the transmit-array weights, and that transmit-array weights (defined here as amplitude and phase states associated with a transmit channel) can be adaptively controlled to maximize the tumor temperature (or microwave power delivered to a tumor), while minimizing the surrounding tissue temperature (or microwave power delivered to the surrounding tissue). It has also been shown that ultrasound receive feedback sensors [13] and a pseudoinverse pattern synthesis method can be used to generate multiple focal points with a phased-array hyperthermia applicator [14, 15]. Other studies [16, 17] and several conference articles [18–20] have investigated the theoretical benefit of using near-field adaptive nulling [21–24] with noninvasive auxiliary dipole sensors to reduce the E-field intensity at selected positions in a target body while maintaining a desired focus at a tumor site. In particular, multiple adaptive E-field nulls were used to show a theoretical reduction in hot spots for a homogeneous elliptical phantom target surrounded by a water bolus and hyperthermia ring array [18–20].

References

1. C.A. Perez and L.W. Brady, *Principles and Practice of Radiation Oncology* (J.B. Lippincott, Philadelphia, 1987).
2. A.W. Guy, "History of Biological Effects and Medical Applications of Microwave Energy," *IEEE Trans. Microw. Theory Tech.* **MTT-32**, 1182 (Sept. 1984).
3. J. Overgaard, "The Effect of Local Hyperthermia Alone and in Combination with Radiation on Solid Tumors," in *Cancer Therapy by Hyperthermia and Radiation, Proc. 2nd Int. Symp., 2–4 June 1997,* ed. C. Streffer (Urban & Schwarzenberg, Baltimore, 1978), pp. 49–61.
4. J. Overgaard, "Clinical Hyperthermia—An Update," *Proc. 8th Int. Congress of Radiation Research* **2**, *Jul. 1987,* eds. E.M. Fielden, J.F. Fowler, J.H. Hendry, and D.O. Scott, p. 942.
5. S.B. Field and J.W. Hand, eds., *An Introduction to the Practical Aspects of Clinical Hyperthermia* (Taylor & Francis, London, 1990).
6. "Special Issue on Cancer Therapy by Electromagnetic Hyperthermia," *J. Microw. Power* **16** (June 1981).
7. "Special Issue on Phased Arrays for Hyperthermia Treatment of Cancer," *IEEE Trans. Microw. Theory Tech.* **MTT-34** (May 1986).
8. "Special Issue on Hyperthermia and Cancer Therapy," *IEEE Trans. Biomed. Eng.* **BME-31** (Jan. 1984).
9. D. Sullivan, "Three-Dimensional Computer Simulation in Deep Regional Hyperthermia Using the Finite-Difference Time-Domain Method," *IEEE Trans. Microw. Theory Tech.* **MTT-38**, 204 (Feb. 1990).
10. R.B. Roemer, K. Hynynen, C. Johnson, and R. Kress, "Feedback Control and Optimization of Hyperthermia Heating Patterns: Present Status and Future Needs," *IEEE Eighth Annual Conf. Eng. Med. Biol. Soc.*, p. 1496 (Nov. 1986).
11. P. Wust, J. Nadobny, R. Felix, P. Deuflhard, A. Louis, and W. John, "Strategies for Optimized Application of Anular-Phased-Array Systems in Clinical Hyperthermia," *Int. J. Hyperthermia* **7**, 157 (Jan.–Feb. 1991).
12. J.W. Strohbehn, E.H. Curtis, K.D. Paulsen, and D.R. Lynch, "Optimization of the Absorbed Power Distribution for an Annular Phased-Array Hyperthermia System," *Int. J. Radiation Oncol. Biol. Phys.* **16**, 589 (1989).
13. E.S. Ebbini, H. Wang, M. O'Donnell, and C.A. Cain, "Acoustic Feedback for Hyperthermia Phased-Array Applicators: Aberration Correction, Motion Compensation, and Multiple Focusing in the Presence of Tissue Inhomogeneities," *Proc. IEEE 1991 Ultrason. Symp.* **2**, 1343 (1991).
14. E.S. Ebbini and C.A. Cain, "Experimental Evaluation of a Prototype Cylindrical Section Ultrasound Hyperthermia Phased-Array Applicator," *IEEE Trans. Ultrason. Ferroelectr. Freq. Control* **38**, 510 (1991).
15. E.S. Ebbini and C.A. Cain, "Multiple-Focus Ultrasound Phased-Array Pattern Synthesis: Optional Driving-Signal Distributions for Hyperthermia," *IEEE Trans. Ultrason. Ferroelectr. Freq. Control* **36**, 540 (1989).
16. A.J. Fenn, "Application of Adaptive Nulling to Electromagnetic Hyperthermia for Improved Thermal Dose Distribution in Cancer Therapy," *Technical Report 917,* Lincoln Laboratory (3 July 1991), DTIC #AD-A241026.
17. A.J. Fenn and G.A. King, "An Adaptive Radio-Frequency Hyperthermia Phased-Array System for Improved Cancer Therapy: Phantom Target Measurements," *Technical Report 999,* Lincoln Laboratory (19 Nov. 1993), ESC-TR-93-299.
18. A.J. Fenn, "Focused Near-Field Nulling for Adaptive Electromagnetic Hyperthermia Applications," *1991 Prog. Electromagn. Res. Symp. Proc. Cambridge, MA, 1–5 July 1991*, p. 393.
19. A.J. Fenn, "Adaptive Hyperthermia for Improved Thermal Dose Distribution," in *Radiation Research: A Twentieth-Century Perspective* **I**: *Congress Abstracts, 7–12 July 1991*, eds. J.D. Chapman, W.C. Dewey, and G.F. Whitmore (Academic Press, San Diego, 1991), p. 290.
20. A.J. Fenn, "Noninvasive Adaptive Nulling for Improved Hyperthermia Thermal Dose Distribution," *IEEE Eng. Med. Biol. Soc. Int. Conf.* **13**, 976 (31 Oct.–3 Nov. 1991).
21. A.J. Fenn, "Theory and Analysis of Near-Field Adaptive Nulling," *1986 Asilomar Conf. on Signals, Systems and Computers* (Computer Society Press of the IEEE, Washington, DC, 1986), pp. 105–109.
22. A.J. Fenn, "Evaluation of Adaptive Phased-Array Antenna Far-Field Nulling Performance in the Near-Field Region," *IEEE Trans. Antennas Propag.* **38**, 173 (1990).
23. A.J. Fenn, H.M. Aumann, F.G. Willwerth, and J.R. Johnson, "Focused Near-Field Adaptive Nulling: Experimental Investigation," *1990 IEEE Antennas Propag. Soc. Int. Symp. Dig.* **1**, 7–11 May 1990, p. 186.
24. A.J. Fenn, "Analysis of Phase-Focused Near-Field Testing for Multiphase-Center Adaptive Radar Systems," *IEEE Trans. Antennas Propag.* **40**, 878 (Aug. 1992).

915 MHz. Experiments were conducted at the University of California at San Francisco (UCSF) Radiation Oncology Department in which the algorithm was used for controlling the hyperthermia array phase shifters to focus the transmitted radiation beam at a hypothetical tumor site in a sugar/saline liquid phantom (dielectric losses of 3 dB/cm). The UCSF experiments are the subject of this article.

Several major differences exist between the SUNY and UCSF experiments. In particular, the hyperthermia equipment used in the two experiments had different transmit frequencies (100 MHz versus 915 MHz) and array geometries (annular versus planar). Because of the difference in transmit frequencies, the SUNY experiments investigated the treatment of deep-seated tumors (depth greater than about 10 cm) while the UCSF experiments were concerned with shallow tumors (depth less than about 3 cm). In addition, the SUNY experiments investigated the use of adaptive nulling as well as adaptive focusing while the UCSF experiments considered just adaptive focusing.

Background

Microwave antenna applicators have frequently been considered for inducing localized hyperthermia to superficial tumors located on the chest wall and head and neck regions. For single-aperture applicators, however, the power-deposition patterns are often limited to effective heating well within the aperture boundaries [15–18]. (Note: The power-deposition patterns are also referred to as the specific absorption rate [SAR], which is equal to $\frac{1}{2}\sigma|E|^2/\rho$, where E is the E-field, σ is the electrical conductivity of the tissue, and ρ is the tissue density.) With 915-MHz microwave radiation, for example, a waveguide applicator has a heating depth limited to less than 3 cm and lateral heating dimensions of 3 to 5 cm—insufficient to treat many tumors [19]. The heating depth is limited

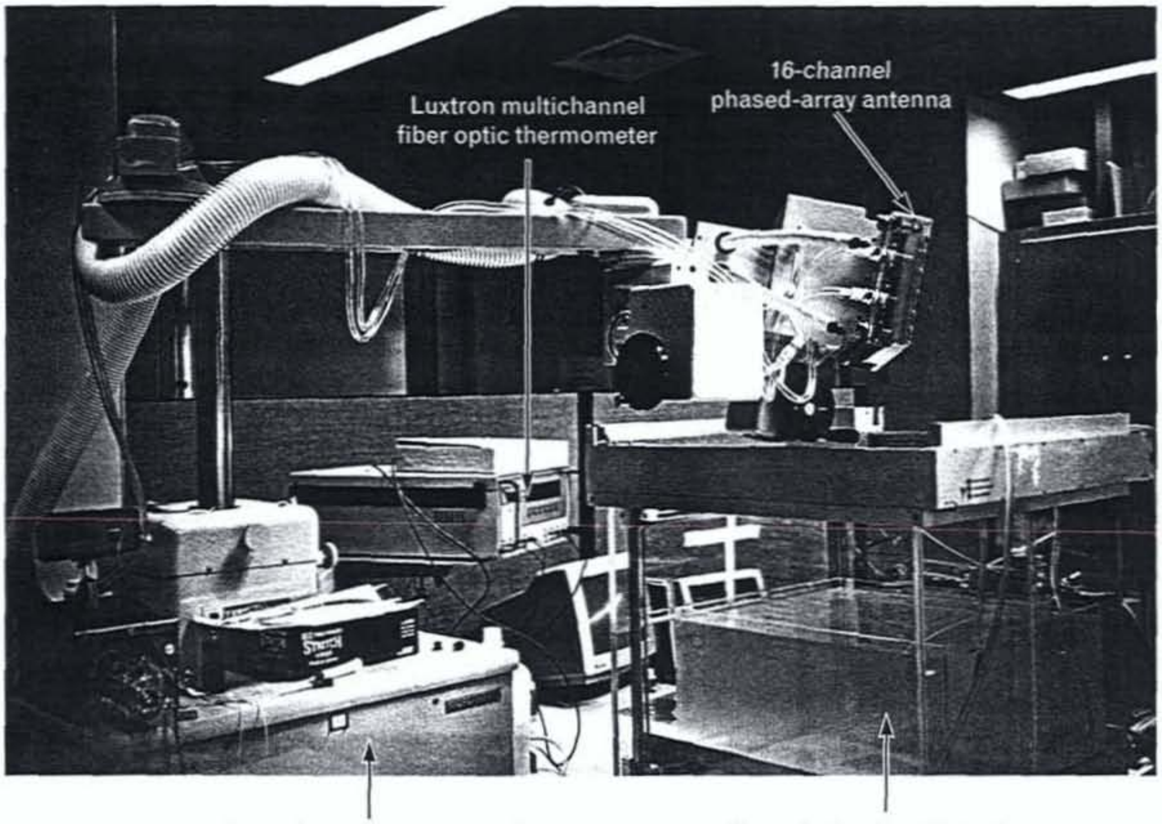

FIGURE 1. The Microtherm-1000 (manufactured by Labthermics Technologies, Inc., of Champaign, Ill.), a 915-MHz microwave planar phased-array hyperthermia system used in experiments at the University of California at San Francisco (UCSF) Radiation Oncology Department.

to only about 3 cm because the dielectric loss of 915-MHz radiation in tissue is typically 3 dB/cm. From previous experiments, researchers have found that a predictor of good local heating control is to use the 50% iso-SAR coverage (laterally and with depth) of the tumor [20].

Several methods for improving the SAR heating patterns of single-aperture hyperthermia devices are under investigation. For example, microwave-absorbing saline-filled boluses can shape the heating pattern of a waveguide applicator, as has been demonstrated in Sherar et al. [21]. Mechanically scanned microwave applicators have also been used to shape the power-deposition pattern [19, 22, 23].

Another method of improving the SAR heating pattern is to use multiple-aperture arrays [24–43]. Researchers have found that phased-array applicators can be used to shape the power-deposition pattern produced by planar [19, 22, 44, 45] and conformal arrays [46, 47]. And studies to improve penetration depth with phased arrays by controlling the phase and amplitude of each array element have been conducted [44, 45, 48].

In our experiments, we have used the Microtherm-1000—a hyperthermia microwave system with 16 antennas (Figure 1) [49]. By transmitting close to the patient with a planar array, the system is able to obtain superficial heating over large (approximately 15×15 cm) as well as small (approximately 3.5×3.5 cm) areas, depending on the array amplitude illumination function. Figure 2 shows the 15×15-cm planar array with its 16 square waveguide elements operating at 915 MHz. The 16 independent variable power amplifiers drive the waveguides, and each of the 16 active channels has an electronically controlled variable-phase shifter to focus the array. A cool-water bolus between the patient and the phased array prevents excess heating of the skin surface. The bolus is filled with circulating deionized water, which has a very low microwave propagation loss of about 0.3 dB/cm.

Previously, UCSF had evaluated (in experiments with phantom materials such as deionized water and muscle-equivalent liquid, and with animals) a systematic-search, iterative focusing algorithm for phased-array control of the Microtherm-1000 [50]. The E-field probe used in the UCSF measurements was a short dipole with a semiconductor diode detector [51–54]. (Note: The Microtherm-1000 currently does not supply E-field probes to monitor clinical hyperthermia treatments; however, as the current measurements indicate, an E-field probe could be added to the system to provide feedback signals to the adaptive algorithm. In theory, with 16 independent transmit channels, the E-field radiation pattern can be controlled at up to 16 points [in the radiation field] by using a feedback signal measured at each point.) In

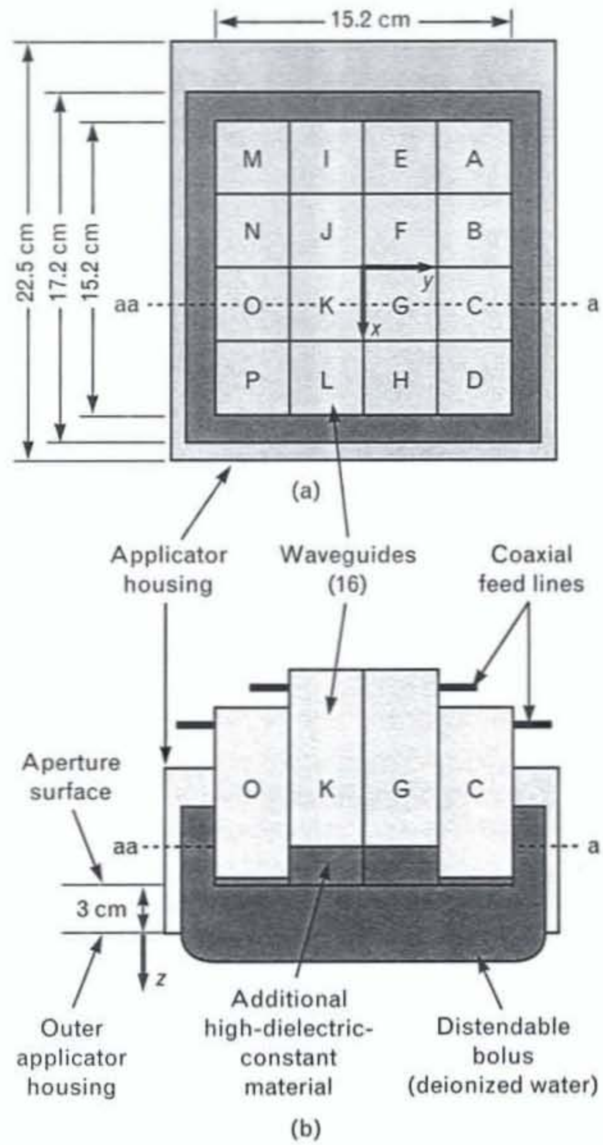

FIGURE 2. The Microtherm-1000 system: (a) footprint and (b) cross section of applicator.

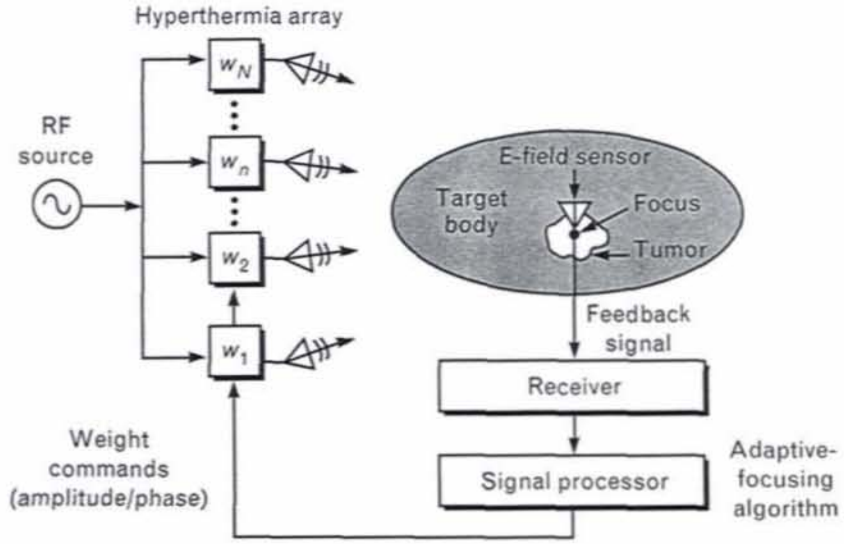

FIGURE 3. Adaptive-focusing hyperthermia system concept.

this article, we investigate an alternative candidate algorithm for the adaptive focusing of the Microtherm-1000. Developed by Lincoln Laboratory, the computer algorithm uses a gradient search based on the maximization of the signal that is received by an E-field sensor positioned within a tumor.

Theory

Adaptive-Focusing Hyperthermia System Concept

The concept of an adaptive-focusing hyperthermia system is shown in Figure 3. To generate the desired E-field distribution with a clinical adaptive hyperthermia system, a field probe is positioned as closely as possible to the tumor site and the hyperthermia array is focused to produce the required field intensity at that site. The probe provides feedback from which the adaptive-array weights w_n can be adjusted to control the amplitudes A and phases ϕ of the individual antenna elements such that the energy received at the tumor site is maximized. (Note: Although Figure 3 shows only one field probe, an array of probes may be used.)

Adaptive Transmit-Array Formulation

Consider a hyperthermia array with N antenna elements (N = 16 for the Microtherm-1000 system). The input signal to each of the N array elements is obtained from the amplitude and phase-adjusted signal distributed by a power divider network. The number of adaptive channels is assumed to be equal to the number of transmit antennas N.

Commonly, the weights are constrained to deliver a required amount of power to the hyperthermia array or the tumor. For simplicity in the experimental adaptive-hyperthermia-array control software, we constrain the weights such that

$$\sum_{n=1}^{N} |w_n|^2 = K,$$

where $|w_n|$ is the transmit-weight magnitude for the nth adaptive channel and K is a constant. To generate an adaptive phase focus, a gradient-search algorithm can be used to control the transmit weights (phase shifters).

Gradient-Search Algorithm

Gradient-search algorithms are commonly used in adaptive-array applications, particularly when the channel-to-channel correlation of the antenna elements cannot be calculated or measured. With a gradient search, only the received power at the E-field probe(s) is measured and used as a feedback signal to the algorithm. Because the Microtherm-1000 system at UCSF measures only the received E-field power, it is appropriate to consider a gradient-search algorithm for the application.

Gradient-search algorithms control the transmit weights iteratively to maximize (focus) the microwave signal received by the field probe(s). Transmit-array phase shifters are adaptively changed in small increments (the process is called dithering) and the received power at the probe(s) is monitored to determine the phase settings that will increase the power most rapidly to a maximum. A wide variety of gradient searches exists [55–60]; in our work we have used a standard method of steepest ascent. The mathematical formulation for the method is straightforward [55, 61]; a detailed description of the formulation in the context of hyperthermia is contained in References 9 and 62.

System Considerations

Figure 4 is a block diagram of an adaptive hyperthermia system controlled by a gradient-search algorithm. Transmit weights $w_{1j}, \ldots, w_{nj}, \ldots, w_{Nj}$ at the jth iteration are shown at the top of the figure. The transmit phased-array antenna induces a voltage across the terminal of the ith receive field-probe antenna. (Note: Figure 4 assumes that the system uses an array of N_{aux} field probes.) For any given configuration of

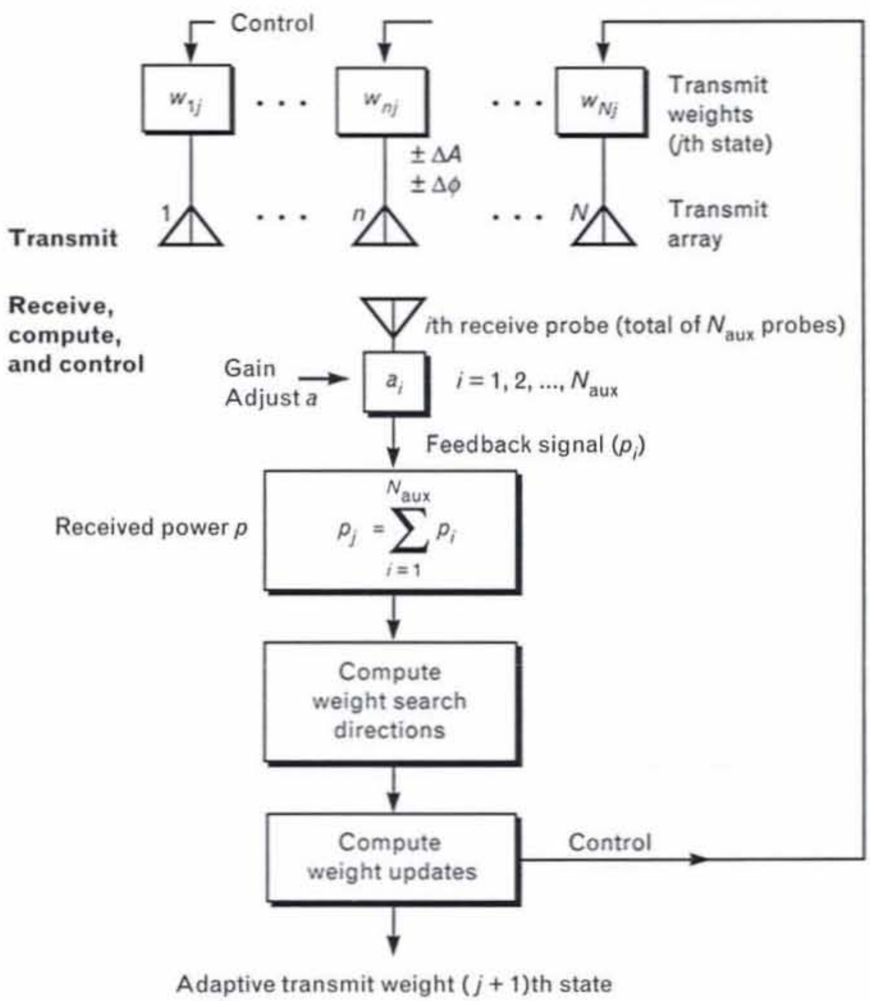

FIGURE 4. Block diagram of gradient-search algorithm for adaptive-focusing hyperthermia system.

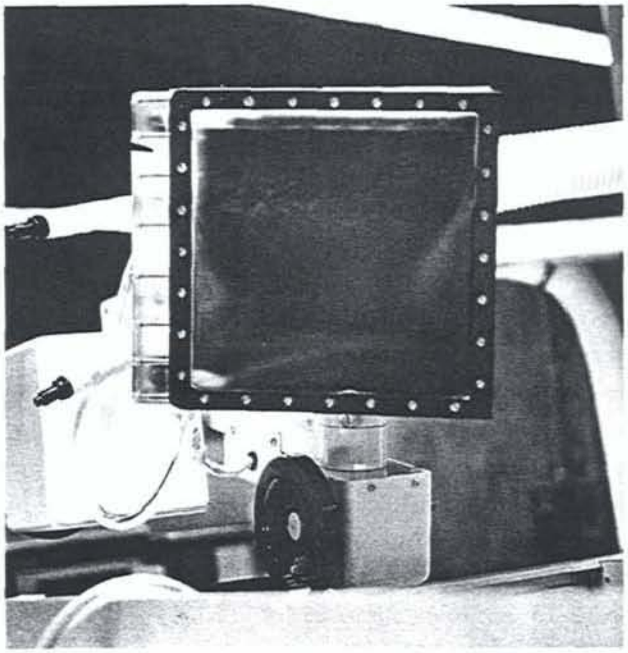

FIGURE 5. The 915-MHz microwave planar phased-array applicator used in the Microtherm-1000.

the transmit weights, each weight is dithered by a small amount in amplitude and phase, and the received power at the ith probe is stored in the computer for calculation of the total received power from the array of N_{aux} probes, the amplitude and phase search directions [62], and the updated $(j + 1)$th transmit-weight configuration. One transmit weight is dithered with the remaining transmit weights in their jth state. The process continues until the $(j + 1)$th weight configuration has converged. Based on other measurements [10, 12] not shown here, convergence for adaptive focusing occurs typically in fewer than about 15 iterations, depending on the gradient-search step size $\Delta\phi$.

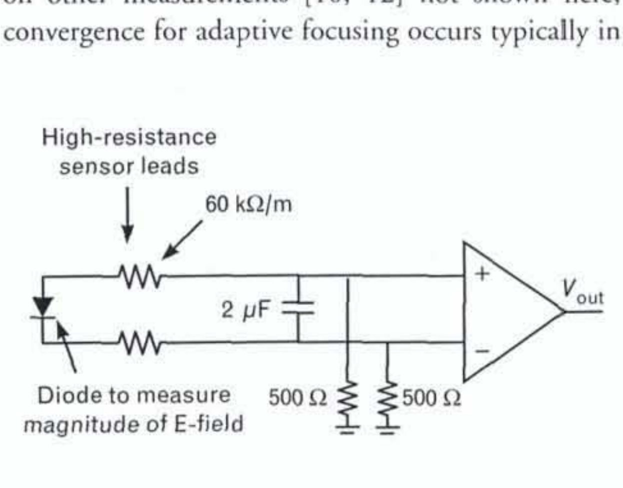

FIGURE 6. Amplifier circuit for E-field probe.

Materials and Methods

The hyperthermia phased-array system used in these measurements is the Labthermics Microtherm-1000 planar phased-array applicator (Figure 1). The system consists of a 15 × 15-cm planar array with a 4 × 4 grid of 16 uniformly spaced square waveguide elements operating at 915 MHz (Figure 2). Figure 5 shows a photograph of the planar phased-array applicator. Because of the water bolus covering the applicator, the actual waveguide radiators of the array are not visible in the photograph. The aperture dimensions of the individual waveguides are 3.8 × 3.8 cm, and the waveguides are filled with a high-dielectric-constant material to provide maximum radiation at 915 MHz. The waveguides are linearly polarized with the dominant E-field component aligned with the y-direction (refer to Figure 2).

The 16 individual waveguides are driven by 16 high-power amplifiers with up to 35-W average power per channel. The power applied to each element is controllable in 10% increments of the adjustable master power level. Each of the 16 active channels has an electronically controlled variable phase shifter (8 bits, 0° to 360°) for focusing the array. The phased-array applicator can be driven in incoherent mode (with 16 independently operating sources with frequencies near 915 MHz) or coherent mode (with a single-frequency generator and independent control of the relative phase of each aperture to within 1.5°). Invasive Luxtron fiber-optic temperature sensors [63] are included with the Microtherm-1000 system to monitor the temperatures obtained during treatment.

To prevent excess heating of a patient's skin surface, the Microtherm-1000 uses a cool-water bolus placed between the patient and the phased array. The bolus consists of deionized water, which has a very low microwave propagation loss, contained within a flexible membrane that can be expanded outward to 6 to 8 cm in front of the applicator face to improve the microwave coupling between the applicator and tissue. The bolus temperature is controlled by circulating cooling water through a thermal-conduction plastic-tubing heat exchanger located in the outer edges

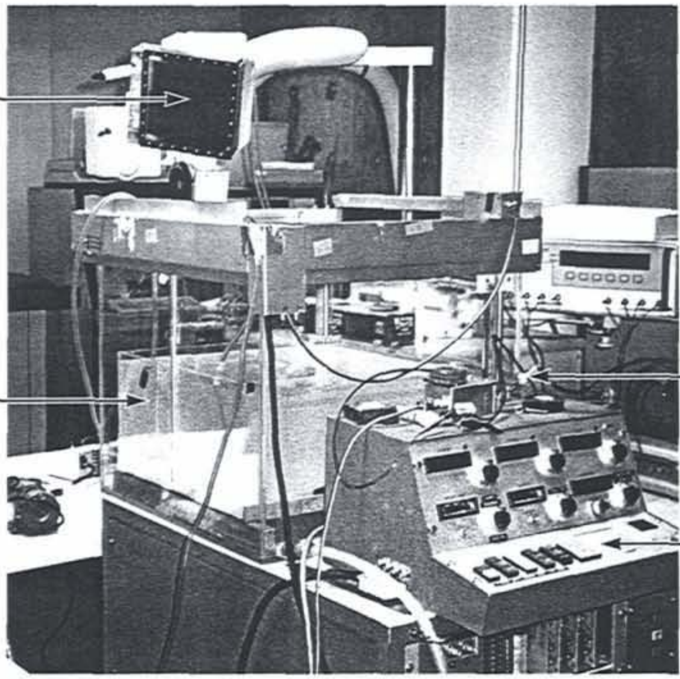

FIGURE 7. Dipole probe, probe (x, y, z) positioner system, and the muscle-equivalent phantom tank.

of the bolus housing. To improve the cooling capacity and transient control of the bolus in the Microtherm-1000, researchers at UCSF replaced the heat exchanger inside the bolus with a closed-circuit pumping system that circulates temperature-controlled deionized water directly through the bolus compartment in series with a heat exchanger mounted in a temperature-regulated water bath.

The E-field probe [51, 52, 54] used in our measurements was fabricated at UCSF and integrated with the Microtherm-1000 system. The E-field sensor is a Schottky detector diode (Hewlett-Packard HP-3486 with an outer diameter of 1.9 mm) with the diode leads arranged to form a dipole antenna of 1 cm length. The sensor is coupled to an amplifier circuit (Figure 6) via high-resistance lead material to minimize perturbation of the fields. (Note: Manufactured by Holaday Industries, the lead material has an outer diameter of 1.2 mm, including the outer insulation.) The rectified DC output voltage is a function of the E-field squared in the orientation of the dipole leads. Figure 7 shows the dipole probe hardware and (x, y, z) positioner. A 12-bit analog-to-digital (A/D) converter samples the E-field probe signal.

In our experiments, we used a liquid muscle-equivalent phantom (sugar and salt dissolved in deionized water) to approximate human tissue. The electrical properties of the phantom (σ = 1.38 Siemens/m and relative permittivity ε_r = 54.7 [64]) were similar to that of high-water-content tissue at 915 MHz (σ = 1.28 Siemens/m and ε_r = 51.0 [65]). The liquid phantom was contained within a 50 × 50 × 22-cm-deep Plexiglas tank, which is shown in Figure 7.

The UCSF hyperthermia array is controlled and monitored by an MS-DOS-based personal computer system with software that implements the gradient-search adaptive-focusing algorithm. The software, developed by Lincoln Laboratory and integrated by UCSF with the Labthermics system, allows the operator to run an adaptive-focusing algorithm that uses the output power of the E-field probe as a feedback signal during the gradient search. The adaptive-focusing algorithm uses only phase control to maximize the E-field at the probe's position.

Measured Results

Review of Earlier Investigations at UCSF

Because of inter-element mutual-coupling effects in the phased array and because of the variation that can

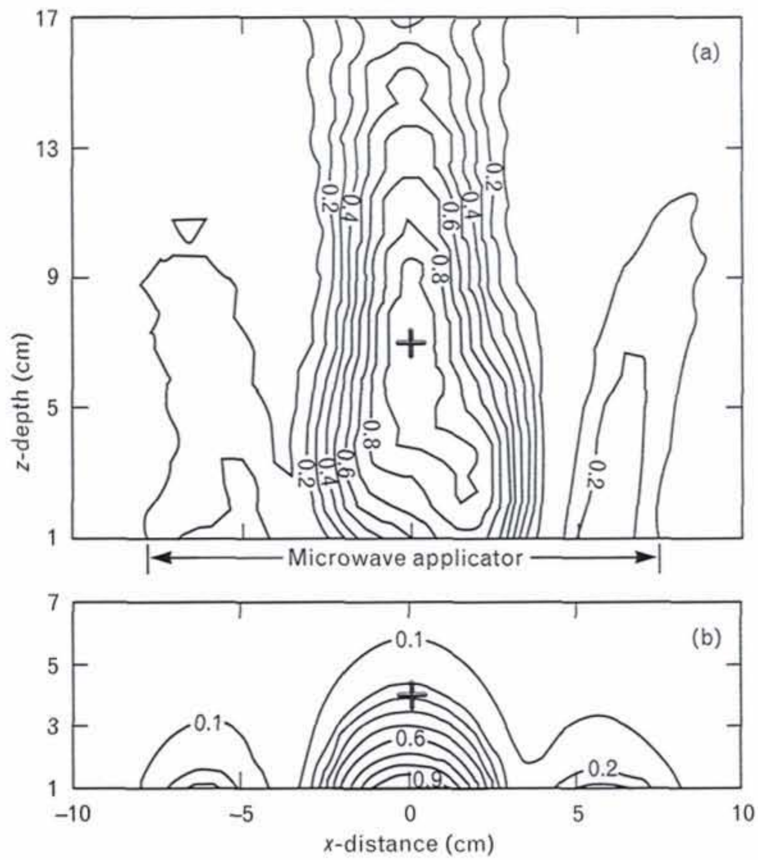

FIGURE 8. Measured E-field radiation pattern for the Microtherm-1000 planar phased array focused at (a) $z = 7$ cm in the deionized-water phantom (propagation loss = 0.3 dB/cm), resulting in a well-focused beam; and at (b) $z = 4$ cm in the muscle-equivalent liquid phantom (propagation loss = 3 dB/cm), resulting in a beam that is not centered at the desired location. In the experiment, the UCSF systematic iterative-search algorithm was used to focus the array. (Note: The radiation pattern contours are shown in 10% power intervals and the location of the focusing probe is indicated with a red "+" sign.)

be expected in phantom materials and humans, it was not possible to select *a priori* the correct phases to focus the Microtherm-1000 [49]. In addition, research was hampered by an inability to calibrate or preset the Microtherm-1000's individual phase shifters accurately to absolute values. Attempts at using theoretically selected phases that were applied to each element produced, at best, marginal results in a water phantom.

To compensate for these problems and to accommodate expected tissue heterogeneities in vivo, a phase selection, or optimization, scheme was developed at UCSF to select the phasing of each transmit channel iteratively for the maximization of the measured SAR at the desired location. A computer/software system linked to the Microtherm-1000 turned on individual elements of the phased array in a predetermined sequence and adjusted the phasing iteratively until a maximum SAR was obtained.

In the process, element F (see Figure 2) is turned on at a 0° phase with all other elements turned off. Next, element K is turned on and adjusted iteratively in phase (from 0° to 360° in 10° increments) to obtain the maximum SAR reading. Element G is then turned on and similarly adjusted until a new maximum SAR reading is obtained. This process continues for the remaining elements in the following sequence: J, B, O, N, C, E, L, H, I, A, P, M, and D. During this systematic iterative-search process, the previously tested elements are kept on at their optimized values while the next element in the sequence is turned on and phase adjusted to maximize the SAR. The entire procedure, from the adjusting of element F through D, takes approximately 1 min to complete. Experiments using this phasing approach have been conducted with different materials: deionized-water, tissue-equivalent liquid phantoms, and a pig thigh [50].

With the UCSF systematic iterative-search algorithm, it was possible to focus the Microtherm-1000 at depths of 7 cm in the deionized-water phantom, as shown in Figure 8(a). (Note: The measured E-field radiation pattern contours in the figure are given in 10% power intervals.) Clearly, maximum radiation occurs in the deionized water in the vicinity of the desired focus. Based on the 50% SAR value, the maximum penetration depth is 15 cm in the deionized-water medium. Using the same algorithm, similar focusing attempts in a muscle-equivalent phantom (Figure 8[b]) did not generate a useful focused beam at depth but produced, in essence, a collimated beam with a beam peak effectively at the surface of the phantom. The data in Figure 8(b) indicate a maximum penetration depth of 3 cm, based on the 50% contour, which reaches $z = 3$ cm.

The microwave propagation loss in deionized water is 0.3 dB/cm, whereas the loss in the muscle-equivalent phantom is close to 3 dB/cm. Clearly the high propagation loss in muscle tissue contributed greatly to the system's inability to focus at the desired depth. Nevertheless, a 3-cm penetration depth is still potentially useful for certain shallow tumors.

The efficacy of the UCSF systematic iterative-search algorithm was also evaluated with a pig thigh in which an implanted SAR sensor was used to optimize the phase. Figure 9 shows the in vivo experimental setup with trial focus positions (at $z = 2.5$ and 4.5 cm) indicated by the shaded circles located on the central axis. In the incoherent mode with the 16 waveguides operating independently, the measured SAR pattern in Figure 10(a) indicates a maximum penetration depth of about 1 cm (for a 50% SAR) on the central axis. This result is consistent with a microwave propagation loss of 3 dB/cm. Figures 10(b) and 10(c) show the measured SAR patterns for a focus at $z = 2.5$ and 4.5 cm, respectively. For the focus at $z = 2.5$ cm, the measured maximum penetration depth (on the principal axis) is 2.3 cm, and the beam peak is at $z = 1$ cm. For the focus at $z = 4.5$ cm, the penetration depth is only 1.9 cm, and the beam peak is at the surface of the target.

Intuitively, one would expect the $z = 4.5$-cm focus to penetrate more deeply than the $z = 2.5$-cm focus, but instead the measurements indicate a reduction in penetration depth when the focus is increased beyond $z = 2.5$ cm. This discrepancy was the principal reason that UCSF was interested in comparing the Lincoln

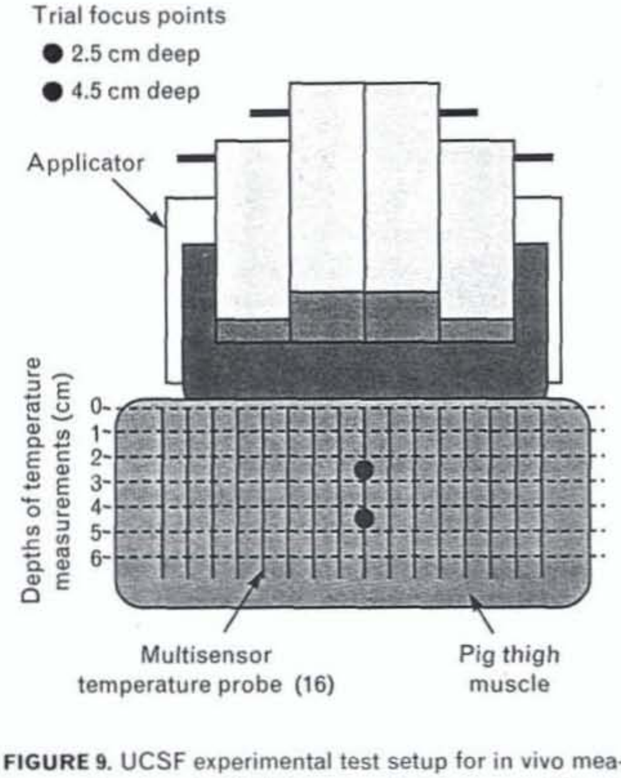

FIGURE 9. UCSF experimental test setup for in vivo measurements of a pig thigh (propagation loss = 3 dB/cm). Note that temperature measurements are taken at numerous sites by 16 multisensor temperature probes spaced 1 cm apart. Each of the 16 probes measures the temperature at 7 different vertical locations spaced 1 cm apart. Thus temperatures within the pig thigh are measured on a 1-cm × 1-cm grid at 112 sites.

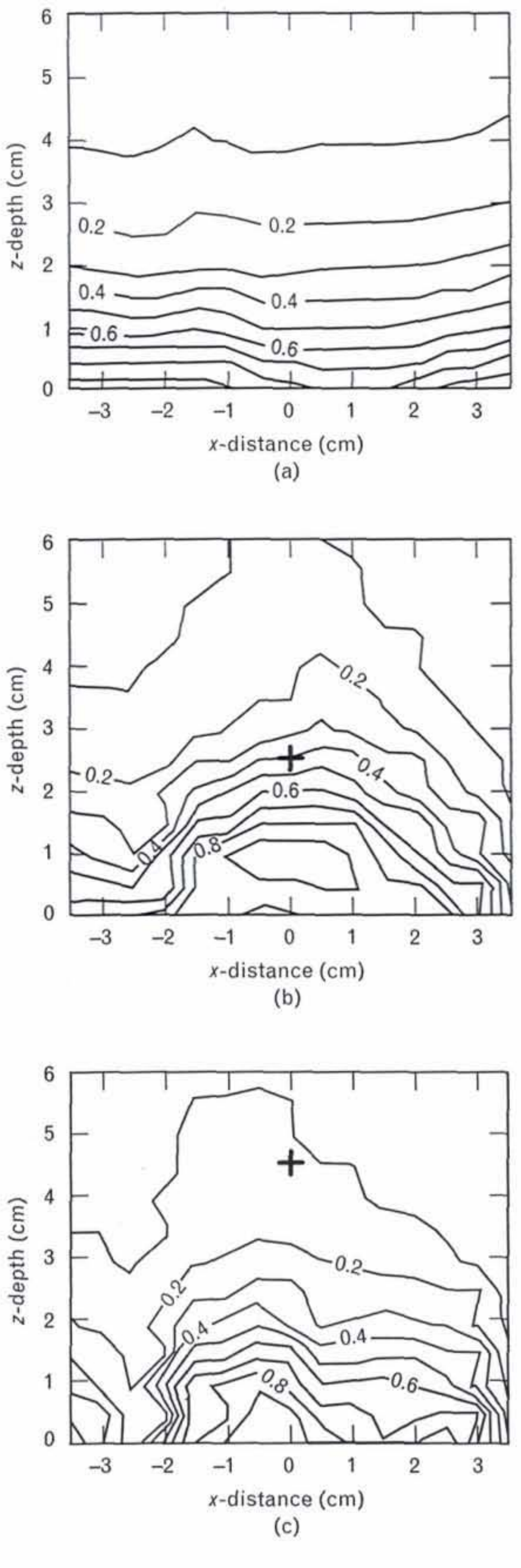

Laboratory gradient-search algorithm with the systematic iterative-search algorithm that had been used.

In Figure 11, the measured SAR is compared with the temperature distribution for the 2.5-cm-focus case (Figure 10[b]), and the two sets of data are consistent. That is, the peak temperature value occurs near the peak of the SAR distribution. (Note: SAR is defined here as $c\Delta T/\Delta t$, where c is the specific heat, and ΔT is the change in temperature over the time interval Δt.)

From the results shown in Figure 8(a), we concluded that the systematic iterative-search algorithm could be used to focus the Microtherm-1000 in a low-loss deionized-water phantom. With the muscle phantom and pig thigh, however, the algorithm did not result in useful focuses (although it did illustrate a possible improvement in penetration depth). Thus one question that remained concerned the effectiveness of the systematic iterative-search algorithm. In particular, we were eager to investigate whether better focusing in a lossy medium could be obtained with an adaptive optimization algorithm, as had been considered previously [7, 10, 12].

New Measurements at UCSF

UCSF and Lincoln Laboratory began collaborating in June 1992 to implement an adaptive-focusing, gradient-search algorithm with the Microtherm-1000. Experiments were performed with the deionized-water and the muscle-equivalent liquid phantoms. Phase focusing was attempted in the central axis of the Microtherm applicator at depths of 6 and 8 cm from the lowest ridge on the applicator housing with an additional 3-cm path length in deionized water from the apertures to this point.

Measured E-field patterns (Figure 12) with the focus set at 8 cm indicate that both optimization

FIGURE 10. Measured specific absorption rate (SAR) for the Microtherm-1000 planar phased array illuminating the pig thigh of Figure 9: (a) incoherent mode with all elements incoherently driven, (b) focused at z = 2.5 cm, and (c) focused at z = 4.5 cm. For parts *b* and *c*, the UCSF systematic iterative-search algorithm was used to focus the array. (Note: SAR is defined here as $c\Delta T/\Delta t$, where c is the specific heat, and ΔT is the change in temperature over the time interval Δt = 30 sec. The location of the focusing probe is indicated with a red "+" sign.)

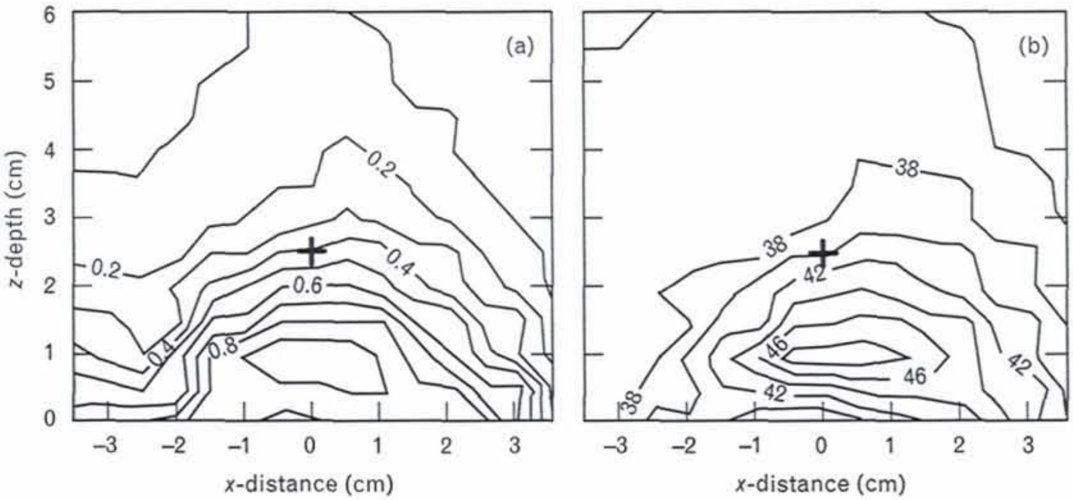

FIGURE 11. Comparison of (a) measured SAR and (b) temperature distributions (given in degrees centigrade for steady-state conditions after 10 min) for the Microtherm-1000 system focused at 2.5 cm in the pig thigh of Figure 9. In the experiment, the UCSF systematic iterative-search algorithm was used to focus the Microtherm-1000. (Note: SAR is defined here as $c\Delta T/\Delta t$, where c is the specific heat, and ΔT is the change in temperature over the time interval $\Delta t = 30$ sec. The location of the focusing probe is indicated with a red "+" sign.)

schemes—the UCSF systematic iterative-search focusing algorithm and the Lincoln Laboratory adaptive gradient-search focusing algorithm—work similarly. Both algorithms result in well-defined focused beams at the desired depths. The current measurements do not consider field mappings in other vertical and horizontal planes. Such additional mappings are necessary to characterize the locations and magnitudes of the E-field sidelobes and possible grating lobes.

It is interesting to note that the radiation patterns in Figure 12 exhibit a z-dependent ripple with spacing approximately equal to 1.8 cm. We suspected that this ripple was caused by a standing-wave pattern created by incident and reflected waves in the phantom water tank. By assuming a dielectric constant of 80 and an electrical conductivity of 0.19 Siemens/m, we calculated the wavelength of 915-MHz microwave radiation in deionized water as 3.6 cm. Thus the ripple spacing was equal to one-half the wavelength, as was expected with a standing-wave pattern.

Measurements in the muscle-equivalent phantom were performed at a depth of 4 cm for three cases of amplitude illumination: equal illumination applied at 100% of the selected power level of 5 W (Figure 13), adjusted uniform illumination with premeasured SAR amplitudes for each element (Figure 14) [49], and inverse-tapered illumination with the application of double the power to the outer elements (Figure 15). These radiation-pattern measurements are similar to those obtained in earlier studies with the UCSF systematic iterative-search algorithm [50]. Note that there are only minor differences between the three radiation patterns of Figures 13 through 15. It is very likely that the four-element group at the center of the array is the dominant contributor to the radiation pattern shape.

Lastly, Figure 16 shows the convergence of the gradient-search steepest-ascent algorithm for the case of the 4-cm focal depth. The measured E-field at the focus has been plotted on the y-axis in power in decibels by computing $10\log(p)$, where p is the value (measured power) of the A/D converter. In the figure, the focal-probe power increases by 17 dB over the 15 iterations with the data indicating convergence in about 7 iterations.

In the experiments, each phase shifter was controlled by an 8-bit D/A converter that had 256 states

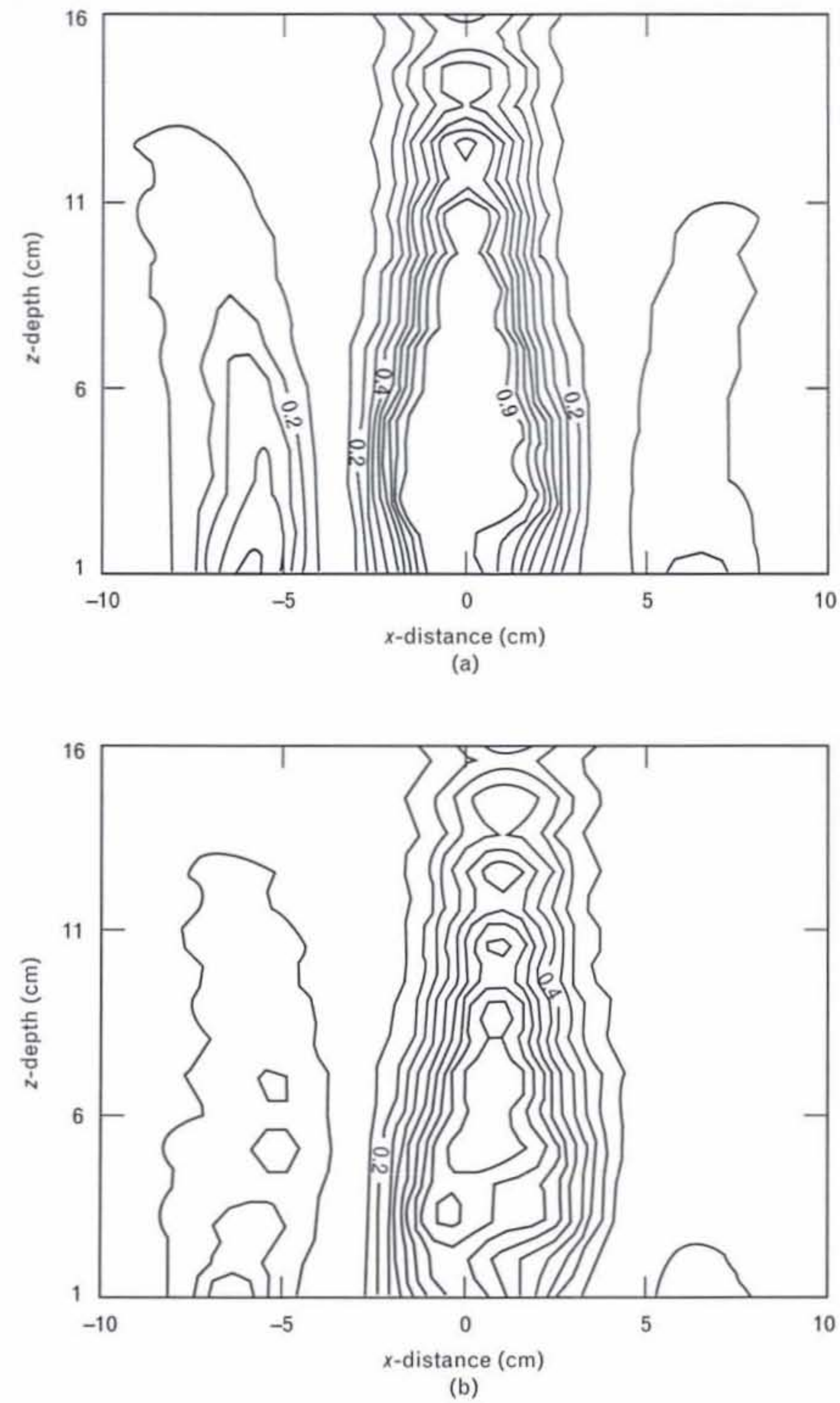

FIGURE 12. Comparison of measured two-dimensional radiation patterns of the Microtherm-1000 with focal depth of 8 cm in deionized-water phantom: (a) UCSF systematic iterative-search focusing algorithm and (b) Lincoln Laboratory adaptive gradient-search focusing algorithm. (Note: The radiation patterns are shown in 10% power levels.)

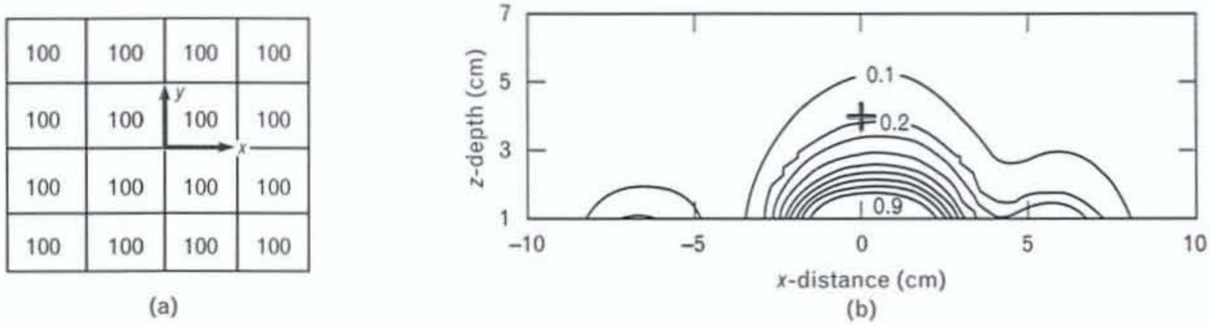

FIGURE 13. Effect of array illumination on radiation pattern for the case of uniform illumination: (a) array illumination (in percent of the selected power level of 5 W) and (b) resulting two-dimensional radiation pattern (in 10% power levels) of the Microtherm-1000 using Lincoln Laboratory adaptive-focusing algorithm with 4-cm focal depth in a muscle-equivalent liquid phantom. Note that the power level of each waveguide is at 100% relative to each other. The location of the focusing probe is indicated with a red "+" sign.

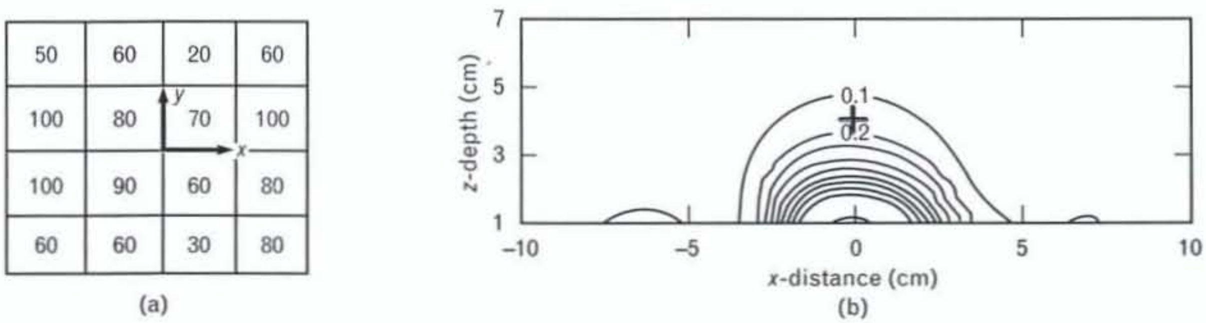

FIGURE 14. Effect of array illumination on radiation pattern for the case of adjusted uniform illumination: (a) array illumination (in percent of the selected power level of 5 W) and (b) resulting two-dimensional radiation pattern (in 10% power levels) of the Microtherm-1000 using Lincoln Laboratory adaptive-focusing algorithm with 4-cm focal depth in a muscle-equivalent liquid phantom. Note that the power level of each waveguide has been adjusted to provide equal amplitude as measured at a receive probe located at the 4-cm depth. The location of the focusing probe is indicated with a red "+" sign.

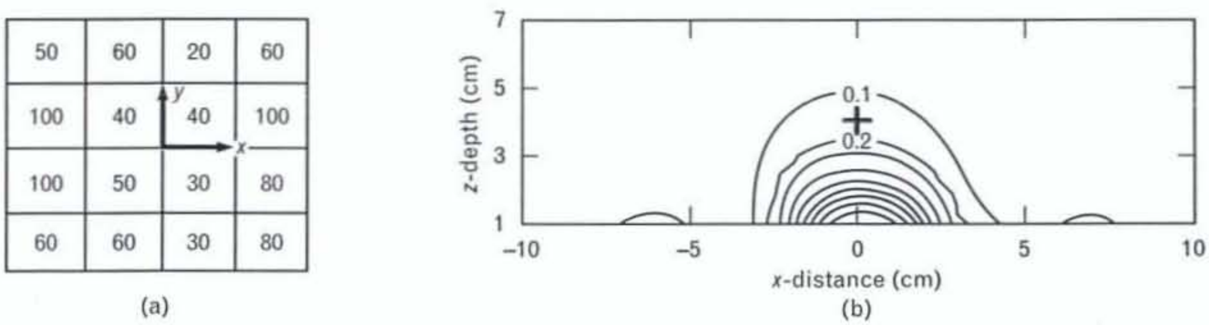

FIGURE 15. Effect of array illumination on radiation pattern for the case of inverse-tapered illumination: (a) array illumination (in percent of the selected power level of 5 W) and (b) resulting two-dimensional radiation pattern (in 10% power levels) of the Microtherm-1000 using Lincoln Laboratory adaptive-focusing algorithm with 4-cm focal depth in a muscle-equivalent liquid phantom. The power level of the outer ring of waveguides has been adjusted to provide twice the power of the inner ring of elements as measured at a receive probe located at the 4-cm depth. The location of the focusing probe is indicated with a red "+" sign.

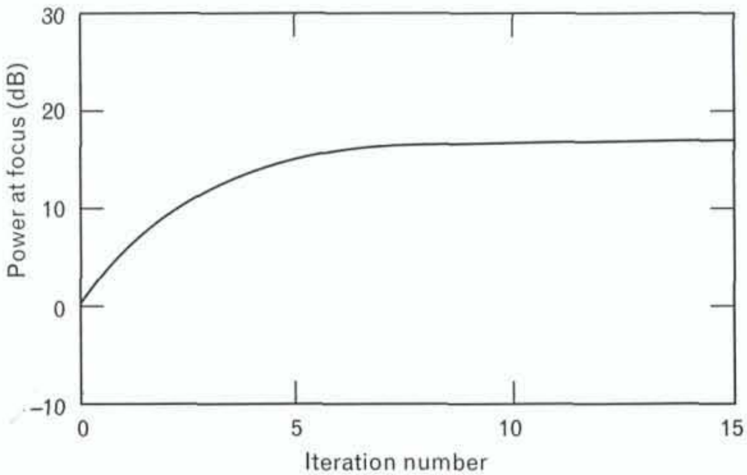

FIGURE 16. Measured E-field focused at $z = 4$ cm as a function of adaptive phase-focusing gradient-search iteration number for a muscle-equivalent liquid phantom. The power level at the focus increases by 17 dB as a result of the Lincoln Laboratory adaptive gradient-search algorithm.

covering a range from 0° to 360°. We chose a maximum step size $\Delta\phi$ equal to five D/A states, which we felt would guarantee convergence and stability of the gradient-search algorithm. Each iteration took less than 1 min to execute; thus the array was focused automatically in less than 10 min, which should be a short enough time for patient therapy. We did not investigate varying the step size $\Delta\phi$, which would have affected the rate of convergence.

The results from these investigations indicate that the low number (16) of array antenna elements, the high attenuation of the signal from the outer elements in the array, and the irregular beam patterns of the individual elements prevent the Microtherm-1000 from producing a well-defined focus in lossy muscle tissue at any appreciable depth beyond 3 cm. Because two proven types of phase-optimization routines—the systematic iterative-search algorithm and the gradient-search algorithm—have yielded similar results, we are confident that the measured data truly depict the best possible performance of the Microtherm-1000 system.

The use of beam shaping and different illumination strategies to improve the penetration depth could be investigated in the future, but significant improvement is not expected. Instead, a better strategy for improving the effective penetration depth might be the use of a curved phased-array applicator with the radiating antenna elements pointed directly toward the focus to provide nearly equivalent path lengths to the focal point from each radiating element. This type of array geometry will be investigated in future measurements.

Conclusion

The power-deposition capabilities of a microwave planar phased-array hyperthermia system using an adaptive-focusing algorithm have been characterized experimentally at the University of California at San Francisco. The measurements shown in this article demonstrate that an adaptive feedback gradient-search focusing computer algorithm developed at Lincoln Laboratory can be used to control the E-field radiation pattern of the Microtherm-1000, a commercial hyperthermia system consisting of a planar phased array with 16 antennas operating at 915 MHz. In our experiments, the algorithm was used to focus the E-field (i.e., maximize the power deposition) of the phased array at a desired target position.

The adaptive algorithm uses a gradient-search feedback technique (method of steepest ascent). In the algorithm, transmit-weight phase dithering is used along with E-field probe power measurements at the desired target position to calculate the required gradient-search directions for sequentially and iteratively focusing all antenna element phase shifters of the array. The algorithm produces two-dimensional radiation patterns that are similar to those produced by a systematic iterative-search algorithm that had been demonstrated previously at UCSF.

E-field focusing is intended to maximize the microwave power delivered to a tumor site relative to the power deposited in surrounding normal tissues. The data presented in this article suggest that this goal can be achieved for shallow tumors (i.e., tumors less than 3 cm beneath the skin surface) with a microwave planar phased-array hyperthermia system using adaptive focusing. Measurements have proven that a planar phased array at 915 MHz can provide a useful focus in lossy muscle tissue (dielectric loss of 3 dB/cm) at a maximum depth of 3 cm.

With the hardware and software modifications implemented at UCSF, the 16-channel 915-MHz Microtherm-1000 system can now serve as a testbed for new types of adaptive phased-array applicators. Future measurements may investigate other types of applicators, for example, a new noninvasive adaptive phased array of monopole antennas operating at 915 MHz (recently designed and fabricated at Lincoln Laboratory [66]). Other non-planar array microwave applicators are under development that should provide much needed geometric flexibility for conforming to contoured body surfaces. Conformable spiral microstrip antennas [46] have been used successfully for superficial heating with noncoherent arrays, but these arrays will very likely prove difficult to focus at depth because of the radiated electric field, which is circularly polarized and has a somewhat higher normal field component. An alternative design of a lightweight, conformable microwave antenna has been reported in Reference 67. Although this antenna also has a complex radiated field with an electric field oriented radially across a circumferential gap and a significant normal field component, this multi-element array has demonstrated phase focusing at depth in preliminary experiments at UCSF [68]. Perhaps most suitable for use as a multi-element conformable array applicator for phase-focused heating at depth is the Current Sheet Applicator design [44, 69], which has a linearly polarized electric field oriented tangential to the body surface for the simplified phasing of adjacent elements.

Acknowledgments

The authors are grateful for their technical discussions with Dr. Everette C. Burdette, formerly of Labthermics Technologies, Inc., and currently with Dornier Medical Systems.

This work was sponsored by the Department of the Air Force and the National Institutes of Health.

REFERENCES

1. M.I. Skolnik, *Introduction to Radar Systems,* 2nd ed. (McGraw-Hill, New York, 1980).
2. R.T. Compton, Jr., *Adaptive Antennas, Concepts and Performance* (Prentice Hall, Englewood Cliffs, NJ, 1988).
3. A. Farina, *Antenna-Based Signal Processing Techniques for Radar Systems* (Artech House, Norwood, MA, 1992).
4. R. Nitzberg, *Adaptive Signal Processing for Radar* (Artech House, Norwood, MA, 1992).
5. A.J. Fenn, "Application of Adaptive Nulling to Electromagnetic Hyperthermia for Improved Thermal Dose Distribution in Cancer Therapy," *Technical Report 917,* Lincoln Laboratory (3 July 1991), DTIC #AD-A241026.
6. A.J. Fenn, "Focused Near-Field Nulling for Adaptive Electromagnetic Hyperthermia Applications," *1991 Prog. Electromagn. Res. Symp. Proc. Cambridge, MA, 1–5 July 1991,* p. 393.
7. A.J. Fenn, "Adaptive Hyperthermia for Improved Thermal Dose Distribution," in *Radiation Research: A Twentieth-Century Perspective* **I**: *Congress Abstracts, 7–12 July 1991,* eds. J.D. Chapman, W.C. Dewey, and G.F. Whitmore (Academic Press, San Diego, 1991), p. 290.
8. A.J. Fenn, "Noninvasive Adaptive Nulling for Improved Hyperthermia Thermal Dose Distribution," *IEEE Eng. Medicine Biol. Soc. Int. Conf.* **13**, 976 (31 Oct.–3 Nov. 1991).
9. A.J. Fenn and G.A. King, "An Adaptive Radio-Frequency Hyperthermia Phased-Array System for Improved Cancer Therapy: Phantom Target Measurements," *Technical Report 999,* Lincoln Laboratory (19 Nov. 1993), ESC-TR-93-299.
10. G.A. King and A.J. Fenn, "Adaptive Nulling Measurements with the BSD Sigma-60 Applicator for Improved Hyperthermia Thermal Distribution," *Sixth Int. Congress on Hyperthermic Oncol.* **1**, *26 Apr.–1 May 1992,* p. 246.
11. A.J. Fenn and G.A. King, "Adaptive Nulling in the Hyperthermia Treatment of Cancer," *Linc. Lab. J.* **5**, 223 (1992).
12. A.J. Fenn and G.A. King, "An Adaptive Radio-Frequency Hyperthermia Phased-Array System for Improved Cancer Therapy: Phantom Target Measurements," to be published in *Int. J. Hyperthermia.*
13. P.F. Turner, T. Schaefermeyer, and T. Saxton, "Future Trends in Heating Technology of Deep-Seated Tumors," *Recent Re-*

sults Cancer Res. **107**, 249 (1988).

14. P.F. Turner, A. Tumeh, and T. Schaefermeyer, "BSD-2000 Approach for Deep Local and Regional Hyperthermia: Physics and Technology," *Strahlentherapie Onkologie* **165**, 738 (1989).
15. G.H. Nussbaum, "Quality Assessment and Assurance in Clinical Hyperthermia: Requirements and Procedures," *Cancer Res. (Suppl.)*, p. 44:4811s (1984).
16. D.L. Denman, M.J. Kolasa, H.R. Elson, B.S. Aron, and J.G. Kereikes, "Specific Absorption Rates in Simulated Tissue Media for a 10 × 10 cm 915-MHz Waveguide Applicator," *Med. Phys.* **14**, 681 (1987).
17. C.K. Chou, J.A. McDougall, K.W. Chan, and K.H. Luk, "Evaluation of Captive Bolus Applicators," *Med. Phys.* **17**, 705 (1990).
18. W.L. Straube, R.J. Myerson, B. Emami, and L.B. Leybovich, "SAR Patterns of External 915-MHz Microwave Applicators," *Int. J. Hyperthermia* **6**, 665 (1990).
19. P. Fessenden, D.S. Kapp, E.R. Lee, and T.V. Samulski, "Clinical Microwave Applicator Design," in *Biological, Physical and Clinical Aspects of Hyperthermia, Medical Physics Monograph 16*, eds. B.R. Paliwal, F.W. Hetzel, and M.W. Dewhirst (American Institute of Physics, New York, 1988), pp. 123–131.
20. C.A. Perez, B. Gillespie, T. Pajak, N. Hornback, B. Emami, and P. Rubin, "Quality Assurance Problems in Clinical Hyperthermia and Its Impact on Therapeutic Outcome: A Report by the Radiation Therapy Oncology Group," *Int. J. Radiation Oncol. Biol. Phys.* **16**, 551 (1989).
21. M.D. Sherar, D.J. Newcombe, W.B. Taylor, and J.W. Hunt, "Investigation of Heating Patterns of the MA-100 and MA-120 Microwave Applicators under Different Water Bolus Arrangements at 915 MHz," in *Radiation Research: A Twentieth-Century Perspective* **I**: *Congress Abstracts, 7–12 July 1991*, eds. J.D. Chapman, W.C. Dewey, and G.F. Whitmore (Academic Press, San Diego, 1991), p. 194.
22. T.V. Samulski, P. Fessenden, E.R. Lee, D.S. Kapp, E. Tanabe, and A. McEuen, "Spiral Microstrip Hyperthermia Applicators: Technical Design and Clinical Performance," *Int. J. Radiation Oncol. Biol. Phys.* **18**, 233 (1990).
23. A. Tennant, J. Conway, and A.P. Anderson, "A Robot-Controlled Microwave Antenna System for Uniform Hyperthermia Treatment of Superficial Tumors with Arbitrary Shape," *Int. J. Hyperthermia* **6**, 193 (1990).
24. "Special Issue on Phased Arrays for Hyperthermia Treatment of Cancer," *IEEE Trans. Microw. Theory Tech.* **MTT-34** (May 1986).
25. "Special Issue on Hyperthermia and Cancer Therapy," *IEEE Trans. Biomed. Eng.* **BME-31** (Jan. 1984).
26. V. Sathiaseelan, M.F. Iskander, G.C.W. Howard, and N.M. Bleehen, "Theoretical Analysis and Clinical Demonstration of the Effect of Power Control Using the Annular Phased-Array Hyperthermia System," *IEEE Trans. Microw. Theory Tech.* **MTT-34**, 514 (1986).
27. V. Sathiaseelan, "Potential for Patient-Specific Optimization of Deep Heating Patterns through Manipulation of Amplitude and Phase," *Strahlentherapie Onkologie* **165**, 743 (1989).
28. D. Sullivan, "Three-Dimensional Computer Simulation in Deep Regional Hyperthermia Using the Finite-Difference Time-Domain Method," *IEEE Trans. Microw. Theory Tech.* **MTT-38**, 204 (1990).
29. B.S. Trembly, A.H. Wilson, M.J. Sullivan, A.D. Stein, T.Z. Wong, and J.W. Strohbehn, "Control of the SAR Pattern within an Interstitial Microwave Array through Variation of Antenna Driving Phase," *IEEE Trans. Microw. Theory Tech.* **MTT-34**, 568 (1986).
30. G. Sato, C. Shibata, S. Sekimukai, H. Wakabayashi, K. Mitsuka, and K. Giga, "Phase-Controlled Circular Array Heating Equipment for Deep-Seated Tumors: Preliminary Experiments," *IEEE Trans. Microw. Theory Tech.* **MTT-34**, 520 (1986).
31. P.A. Cudd, A.P. Anderson, M.S. Hawley, and J. Conway, "Phased-Array Design Considerations for Deep Hyperthermia through Layered Tissue," *IEEE Trans. Microw. Theory Tech.* **MTT-34**, 526 (1986).
32. N. Morita, T. Hamasaki, and N. Kumagai, "An Optimal Excitation Method in Multiapplicator Systems for Forming a Hot Zone inside the Human Body," *IEEE Trans. Microw. Theory Tech.* **MTT-34**, 532 (1986).
33. C. De Wagter, "Optimization of Simulated Two-Dimensional Temperature Distributions Induced by Multiple Electromagnetic Applicators," *IEEE Trans. Microw. Theory Tech.* **MTT-34**, 589 (1986).
34. M. Knudsen and U. Hartmann, "Optimal Temperature Control with Phased-Array Hyperthermia System," *IEEE Trans. Microw. Theory Tech.* **MTT-34**, 597 (1986).
35. C.F. Babbs, V.A. Vaguine, and J.T. Jones, "A Predictive-Adaptive, Multipoint Feedback Controller for Local Heat Therapy of Solid Tumors," *IEEE Trans. Microw. Theory Tech.* **MTT-34**, 604 (1986).
36. R.B. Roemer, "Physical and Engineering Aspects of Hyperthermia," *Proc. 8th Int. Congress Radiation Res.* **2**, *July 1987*, eds. E.M. Fielden, J.F. Fowler, J.H. Hendry, and D.O. Scott, p. 948.
37. R.B. Roemer, K. Hynynen, C. Johnson, and R. Kress, "Feedback Control and Optimization of Hyperthermia Heating Patterns: Present Status and Future Needs," *IEEE Eighth Annual Conf. Eng. Med. Biol. Soc., Nov. 1986*, p. 1496.
38. R.B. Roemer, "Optimal Power Deposition in Hyperthermia. I. The Treatment Goal: The Ideal Temperature Distribution: The Role of Large Blood Vessels," *Int. J. Hyperthermia* **7**, 317 (1991).
39. A. Boag and Y. Leviatan, "Optimal Excitation of Multiapplicator Systems for Deep Regional Hyperthermia," *IEEE Trans. Biomed. Eng.* **BME-37**, 987 (1990).
40. P. Wust, J. Nadobny, R. Felix, P. Deuflhard, A. Louis, and W. John, "Strategies for Optimized Application of Annular-Phased-Array Systems in Clinical Hyperthermia," *Int. J. Hyperthermia* **7**, 157 (1991).
41. D.B. Nguyen and J.W. Strohbehn, "Optimal Positions, Orientations, Amplitudes and Phases of Movable Microwave Applicators in Hyperthermia Treatment," in *Hyperthermic Oncol. 1988* **1**, eds. T. Sugahara and M. Saito (Taylor & Francis, London, 1989), pp. 738–739.
42. J.W. Strohbehn, E.H. Curtis, K.D. Paulsen, and D.R. Lynch, "Optimization of the Absorbed Power Distribution for an Annular Phased-Array Hyperthermia System," *Int. J. Radiation Oncol. Biol. Phys.* **16**, 589 (1989).
43. J.T. Loane III and S.W. Lee, "Gain Optimization of a Near-Field Focusing Array for Hyperthermia Applications," *IEEE Trans. Microw. Theory Tech.* **MTT-37**, 1629 (1989).
44. M.K. Gopal, J.W. Hand, M.L.D. Lumori, S. Alkhairi, K.D. Paulsen, and T.C. Cetas, "Current Sheet Applicator Arrays for Superficial Hyperthermia of Chest Wall Lesions," *Int. J. Hyperthermia* **8**, 227 (1992).
45. H.R. Underwood, A.F. Peterson, and R.L. Magin, "Electric-Field Distribution Near Rectangular Microstrip Radiators for Hyperthermia Heating: Theory versus Experiment in Water," *IEEE Trans. Biomed. Eng.* **39**, 146 (1992).
46. E.R. Lee, T.R. Wilsey, P. Tarczy-Hornoch, D.S. Kapp, P.

Fessenden, A. Lohrbach, and S. Prionas, "Body Conformable 915 MHz Microstrip Array Applicators for Large Surface Area Hyperthermia," *IEEE Trans. Biomed. Eng.* **39**, 470 (1992).

47. D.S. Kapp, P. Fessenden, T.V. Samulski, M.A. Bagshaw, R.S. Cox, E.R. Lee, A.W. Lohrbach, J.L. Meyer, and S.D. Prionas, "Stanford University Institutional Report. Phase I Evaluation of Equipment for Hyperthermia Treatment of Cancer," *Int. J. Hyperthermia* **4**, 75 (1988).
48. J.W. Hand, J.L. Cheetham, and A.J. Hind, "Absorbed Power Distributions from Coherent Microwave Arrays for Localized Hyperthermia," *IEEE Trans. Microw. Theory Tech.* **MTT-34**, 484 (1986).
49. C.J. Diederich and P.R. Stauffer, "Pre-Clinical Evaluation of a Microwave Planar Array Applicator for Superficial Hyperthermia," *Int. J. Hyperthermia* **9**, 227(1993).
50. C.J. Diederich, G. Sherwin, C. Adams, and P.R. Stauffer, "Evaluation of a Multi-Element Microwave Applicator for Hyperthermia," in *Radiation Research: A Twentieth-Century Perspective* **I**: *Congress Abstracts, 7–12 July 1991*, eds. J.D. Chapman, W.C. Dewey, and G.F. Whitmore (Academic Press, San Diego, 1991), p. 194.
51. H.I. Bassen, M. Swicord, and J. Abita, "A Miniature Broad-Band Electric Field Probe," *Annals of the New York Academy of Sciences, Biological Effects of Nonionizing Radiation* **247**, 481 (1975).
52. H.I. Bassen and G.S. Smith, "Electric Field Probes—A Review," *IEEE Trans. Antennas Propag.* **AP-31**, 710 (Sept. 1983).
53. A. Uhlir, "Characterization of Crystal Diodes for Low-Level Microwave Detection," *Microw. J.* **6**, 59 (July 1963).
54. C.H. Durney and M.F. Iskander, "Antennas for Medical Applications," in *Antenna Handbook: Theory, Applications, and Design*, eds. Y.T. Lo and S.W. Lee (Van Nostrand Reinhold, New York, 1988).
55. R.L. Zahradnik, *Theory and Techniques of Optimization for Practicing Engineers* (Barnes and Noble, New York, 1971), pp. 118–124.
56. L. Hasdorff, *Gradient Optimization and Nonlinear Control* (John Wiley, New York, 1976).
57. D.J. Farina and R.P. Flam, "A Self-Normalizing Gradient-Search Adaptive Array Algorithm," *IEEE Trans. Aerosp. Electron. Syst.* **27**, 901 (1991).
58. A. Cantoni, "Application of Orthogonal Perturbation Sequences to Adaptive Beamforming," *IEEE Trans. Antennas Propag.* **AP-28**, 191 (1980).
59. L.C. Godara and A. Cantoni, "Analysis of the Performance of Adaptive Beam Forming Using Perturbation Sequences," *IEEE Trans. Antennas Propag.* **AP-31**, 268 (1983).
60. D.C. Farden and R.M. Davis, "Orthogonal Weight Perturbation Algorithms in Partially Adaptive Arrays," *IEEE Trans. Antennas Propag.* **AP-33**, 56 (1985).
61. A.J. Fenn, "Maximizing Jammer Effectiveness for Evaluating the Performance of Adaptive Nulling Array Antennas," *IEEE Trans. Antennas Propag.* **AP-33**, 1131 (Oct. 1985).
62. A.J. Fenn, C.J. Diederich, and P.R. Stauffer, "Experimental Evaluation of an Adaptive Focusing Algorithm for a Microwave Planar Phased-Array Hyperthermia System at UCSF," *Technical Report 977*, Lincoln Laboratory (17 May 1993), ESC-TR-92-203.
63. T.V. Samulski and E.R. Lee, "Preclinical Evaluation of Luxtron 3000 System," *IEEE Eighth Annual Conf. Eng. Med. Biol. Soc., Fort Worth, TX, 7–10 Nov. 1986*, p. 1493.
64. G. Hartsgrove, A. Kraszewski, and A. Surowiec, "Simulated Biological Materials for Electromagnetic Radiation Absorption Studies, *Bioloelectromagnetics* **8**, 29 (1987).
65. J.W. Hand, "Biophysics and Technology of Electromagnetic Hyperthermia," in *Methods of External Hyperthermic Heating*, ed. M. Gautherie (Springer-Verlag, Berlin, 1990), pp. 1–59.
66. A.J. Fenn, D.S. Poe, C.E. Reuter, and A. Taflove, "Noninvasive Monopole Phased Array for Hyperthermia Treatment of Cranial-Cavity and Skull-Base Tumors: Design, Analysis, and Phantom Tests," *IEEE Annual Conf. Eng. Med. Biol. Soc., San Diego, CA* **15**, part 3, p. 1453 (1993).
67. P.R. Stauffer, C.J. Diederich, and D. Bozzo, "Radial E-Field Microwave Antenna for Superficial Hyperthermia via Single or Multi-Element Conformal Apertures," *Sixth Int. Congress of Hyperthermic Oncology* **1**, ed. E.W. Gerner, p. 319 (1992).
68. P.R. Stauffer and C.J. Diederich, "915 MHz Conformal Array Microwave Applicator," *Proc. North American Hyperthermia Soc. Mtg., Dallas, TX*, p. 13 (1993).
69. M.K. Gopal and T.C. Cetas, "Current Sheet Applicators for Clinical Microwave Hyperthermia," *IEEE Trans. Microw. Theory Tech.* **MTT-41**, 431 (1993).

ALAN J. FENN
received the following degrees in electrical engineering: a B.S. in 1974 from the University of Illinois in Chicago and an M.S. and Ph.D. in 1976 and 1978, respectively, from Ohio State University in Columbus.

From 1974 to 1978, Alan was a graduate research associate at the Ohio State University ElectroScience Laboratory, where he did research in phased-array antenna analysis. He later became a senior engineer at Martin Marietta Aerospace in Denver, where he was involved in broadband antenna research and development from 1978 to 1981. He joined the staff of Lincoln Laboratory in 1981 and was a member of the Space Radar Technology Group from 1982 to 1991, where his research was in phased-array antenna design, adaptive-array near-field testing, and antenna and radar cross-section measurements. Since 1990 he has been conducting research in the application of adaptive-nulling techniques to radio frequency (RF) hyperthermia treatment. He is currently an assistant leader in the RF Technology Group, where he is investigating optoelectronic integrated-circuit phased-array antennas for mobile satellite communications applications.

In 1990 Alan was a corecipient of the IEEE Antennas & Propagation Society's H.A. Wheeler Applications Prize Paper Award for "Phased Array Antenna Calibration and Pattern Prediction Using Mutual Coupling Measurements," a paper that he coauthored for the *IEEE Transactions on Antennas and Propagation.* He served as an associate editor in the area of adaptive arrays for the *IEEE Transactions on Antennas and Propagation* from 1989 to 1991. He is a senior member of the IEEE and a member of the North American Hyperthermia Society, and has been appointed to a five-year term of membership in the Institute for Systems and Components of the Electromagnetics Academy.

He is the author or coauthor of more than 20 articles in his field and has presented more than 20 papers at national and international society meetings.

CHRIS J. DIEDERICH
received a B.S. degree in bioengineering from the University of California, San Diego, in 1984, and an M.S. and a Ph.D. degree in electrical engineering from the University of Arizona in 1986 and 1990, respectively. He is an assistant adjunct professor at the University of California, San Francisco, Radiation Oncology Department, where his focus of research has been on the design and development of hyperthermia devices and other thermal therapy delivery systems. Chris is a member of the North American Hyperthermia Society.

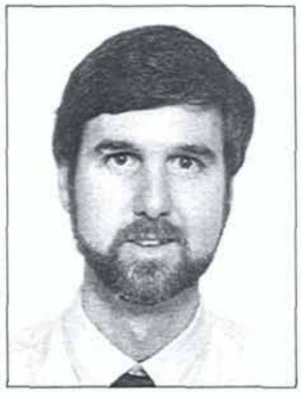

PAUL R. STAUFFER
received a B.A. degree in physics from the College of Wooster in 1975 and an M.S. degree in electrical engineering from the University of Arizona in 1979. He is an associate adjunct professor at the University of California, San Francisco, Radiation Oncology Department, where his focus of research has been on the engineering development of RF, microwave, and ultrasound hyperthermia technologies. He has received a clinical engineering certification from the International Certification Commission and a medical physics certification in hyperthermia from the American Board of Medical Physics. He is a member of the North American Hyperthermia Society.